Fuel Cells

DOI: 10.1002/ange.201303025

Optimized Synthesis of Fe/N/C Cathode Catalysts for PEM Fuel Cells: A Matter of Iron–Ligand Coordination Strength**

Juan Tian, Adina Morozan, Moulay Tahar Sougrati, Michel Lefèvre, Régis Chenitz, Jean-Pol Dodelet, Deborah Jones, and Frédéric Jaouen**

Hydrogen–air polymer-electrolyte-membrane fuel cells (PEMFCs) show promise for the replacement of gasoline internal-combustion engines for vehicle propulsion and other applications. However, the high cost of components, which is largely due to the use of platinum-based catalysts for the O_2-reduction reaction (ORR), remains an impediment.[1] For a production of 500 000 PEMFC stacks a year, electrocatalysts alone were estimated to account for nearly half the cost of a stack.[2]

Recent studies on pyrolyzed Fe/nitrogen/carbon and Co/nitrogen/carbon catalysts for the ORR have increased their initial performance close to the level reached by platinum-based catalysts, and other studies have demonstrated promising durability.[3] We reported the use of a Zn^{II} zeolitic imidazolate framework (ZIF) as a microporous support for ferrous acetate ($Fe^{II}Ac_2$) and 1,10-phenanthroline to prepare a catalyst precursor which, after pyrolysis in Ar and then in NH_3, resulted in unprecedented activity and power performance.[4] The investigated ZIF, referred to as ZIF-8, was a commercial product (Basolite Z1200 from BASF). ZIFs are a subclass of metal–organic frameworks (MOFs), which were first used for the preparation of platinum-free catalysts by Liu and co-workers.[5] MOFs are now actively investigated for electrochemical applications.[6]

Herein, we describe our investigations on the replacement of 1,10-phenanthroline (phen) with 2,4,6-tris(2-pyridyl)-*s*-triazine (TPTZ) in our synthesis with ZIF-8. The use of TPTZ was investigated previously by Zhang and co-workers, who used a high-surface-area carbon material as a host.[7] However, the current density in the resulting PEMFC was only approximately 0.1 $A\,cm^{-2}$ at 0.6 V,[7c] as compared to the value of 1.2 $A\,cm^{-2}$ observed with Fe/phen/ZIF-8 precursors.[4] We show herein that a high performance can also be reached with TPTZ by the use of an appropriate synthesis procedure based on an improved understanding of the coordination chemistry of the Fe^{II}/ligand/ZIF-8 catalyst precursor.

We first prepared an Fe/TPTZ/ZIF-8 catalyst precursor of weight composition 1:10:90 (see the Supporting Information) by wet impregnation followed by drying and planetary ball milling. This composition results in a TPTZ/Fe molar ratio of about 2:1. The blue color characteristic of $[Fe^{II}(TPTZ)_2]$ was immediately observed when $Fe^{II}Ac_2$ and TPTZ were dissolved. ZIF-8 was then dispersed in the solution, whose color slowly changed to gray-blue and then ochre. The absorption peak at 596 nm characteristic of $[Fe^{II}(TPTZ)_2]$[8] was no longer observed in the UV/Vis spectrum after 2 h (Figure 1 a). Thus, $[Fe(TPTZ)_2]$ had reacted with ZIF-8. We expected 2-methyl-imidazole (2-MeIm), the structuring ligand of ZIF-8, to compete with TPTZ for ferrous cations. Indeed, the absorption peak of $[Fe(TPTZ)_2]$ also vanished after the addition of 2-MeIm (see Figure S1 in the Supporting Information). In contrast, this competition for Fe^{II} cations between 2-MeIm of ZIF-8 and the phen ligand was not observed for the Fe/phen/ZIF-8 system. The absorption peak at 510 nm and red color characteristic of $[Fe^{II}(phen)_3]$[9] were retained after the addition of ZIF-8 (Figure 1 b).

The iron coordination was further investigated by Fe^{57} Mössbauer spectroscopy, a technique based on the recoil-free absorption of γ rays by Fe^{57} nuclei. The Mössbauer spectrum of Fe/TPTZ after the wet impregnation and air drying of $Fe^{II}Ac_2$ and TPTZ corresponded to $[Fe^{II}(TPTZ)_2]$ (Figure 2 a).[10a] Doublets a1 and a2 were unambiguously assigned to high-spin Fe^{II} owing to the high value of the center position between the two peaks, the so-called isomer shift (IS; see Table S1 in the Supporting Information). The peak-to-peak separation (quadrupole splitting, QS) was 2.45 and 2.05 $mm\,s^{-1}$ for a1 and a2, respectively (see Table S1). Next, the Mössbauer spectrum of Fe/2-MeIm after the wet impregnation and air drying of $FeAc_2$ and 2-MeIm (Figure 2 b) could be assigned to low-spin Fe^{II} coordinated by 2-MeIm (IS: 0.32 $mm\,s^{-1}$, QS: 0.68 $mm\,s^{-1}$).[10b] The ferrous state is further supported by the QS values reported for $[Fe^{III}(TPTZ)]$ (0.97 $mm\,s^{-1}$) and $[Fe^{III}(2\text{-MeIm})]$ (2.2–2.5 $mm\,s^{-1}$).[10] These values do not match our experimental data (Figure 2 a,b; see also Table S1). Figure 2 c shows the spectrum for Fe/TPTZ/ZIF-8 after wet impregnation, drying, and planetary ball milling. It was fitted with two doublets with IS values of 0.33 and 0.39 $mm\,s^{-1}$ and QS values of 0.31 and 0.87 $mm\,s^{-1}$. These parameters do not match those of $[Fe^{II}(TPTZ)_2]$, and the possible assignment of doublet c2 to $[Fe^{III}(TPTZ)]$ can also be discarded, since this complex shows an asymmetric doublet characteristic of high-spin Fe^{III} complexes.[10b] The two doublets in Figure 2 c have parameters similar to those

[*] Dr. J. Tian, Dr. M. Lefèvre, Dr. R. Chenitz, Prof. J.-P. Dodelet
Institut National de la Recherche Scientifique Energie, Matériaux et Télécommunications
1650 boulevard Lionel Boulet, Varennes (Qc) J3X 1S2 (Canada)
E-mail: dodelet@emt.inrs.ca

Dr. A. Morozan, Dr. M. T. Sougrati, Dr. D. Jones, Dr. F. Jaouen
Université Montpellier 2, Institut Charles Gerhardt Montpellier
2 place Eugène Bataillon, 34095 Montpellier (France)
E-mail: frederic.jaouen@univ-montp2.fr

[**] We acknowledge funding by the NSERC, and by the ANR under contract 2011 CHEX 004 01. PEM = polymer electrolyte membrane.

Supporting information for this article is available on the WWW under http://dx.doi.org/10.1002/anie.201303025.

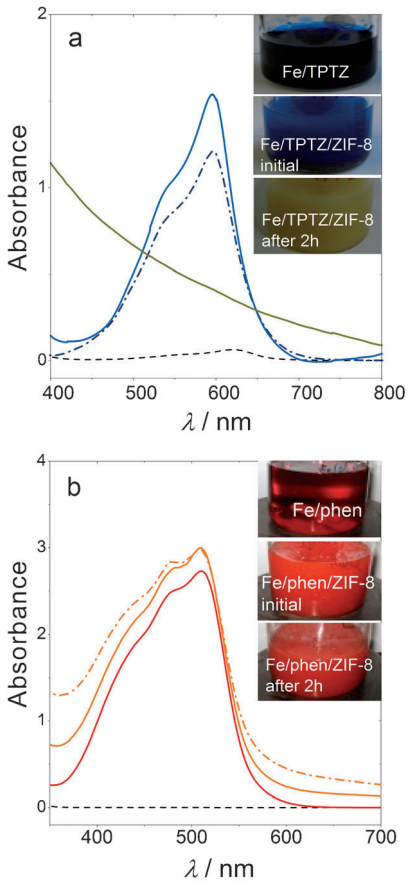

Figure 1. a) UV/Vis spectra for Fe/TPTZ/ZIF-8. Dashed black curve: TPTZ; dot-dashed blue curve: Fe/TPTZ (molar ratio 1:2); solid blue curve: Fe/TPTZ/ZIF-8 of composition 1:10:90 just after the addition of ZIF-8; ochre curve: Fe/TPTZ/ZIF-8 (1:10:90) 2 h after the addition of ZIF-8. b) UV/Vis spectra for Fe/phen/ZIF-8. Dashed black curve: phen; solid red curve: Fe/phen (molar ratio 1:3); solid orange curve: Fe/phen/ZIF-8 of composition 1:10:90 just after the addition of ZIF-8; dot-dashed orange curve: Fe/phen/ZIF-8 (1:10:90) 2 h after the addition of ZIF-8.

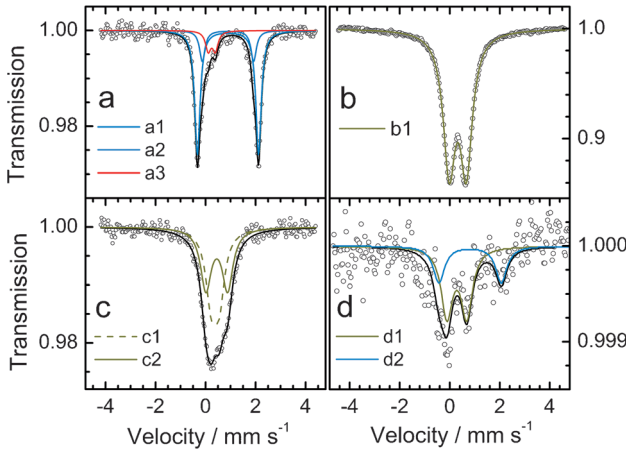

Figure 2. Mössbauer spectra for a) Fe/TPTZ (molar ratio 1:3) and b) Fe/2-MeIm (molar ratio 1:3) after wet impregnation and drying, c) Fe/TPTZ/ZIF-8 (1:10:90) after wet impregnation, drying, and planetary ball milling (precursor of catalyst A), and d) Fe/TPTZ/ZIF-8 (1:10:90) after direct planetary ball milling (precursor of catalyst C). Mass of Fe for Mössbauer measurements: a) 2.1 $mg_{Fe}\,cm^{-2}$, b) 5.0 $mg_{Fe}\,cm^{-2}$, c) 1.6 $mg_{Fe}\,cm^{-2}$, d) 0.8 $mg_{Fe}\,cm^{-2}$.

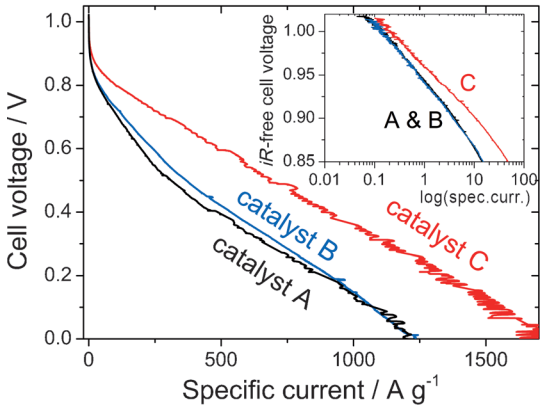

Figure 3. Effect of the method used to prepare the catalyst precursor on fuel-cell performance. The uncorrected cell voltage is plotted against the specific current of the cathode catalyst. In the insert, the *iR*-free cell voltage is plotted against the logarithm of the specific current. The cathode loading was 1 $mg\,cm^{-2}$ (1000 $A\,g^{-1} \equiv 1\,A\,cm^{-2}$), the anode contained 0.5 $mg_{Pt}\,cm^{-2}$, and the membrane was Nafion 117. The experiments were carried out at 80 °C under O_2/H_2 at a relative humidity of 100% and a gauge pressure of 1 bar.

reported for $[Fe^{II}(2\text{-MeIm})]$.[10b] Thus, doublets c1 and c2 were assigned to Fe^{II} coordinated to 2-MeIm ligands of ZIF-8. The same assignment was made for doublets e1 and e2 observed for Fe/ZIF-8 obtained by the wet impregnation, drying, and planetary ball milling of $Fe^{II}Ac_2$ and ZIF-8 (see Figure S2). The presence of two doublets was attributed to two types of coordination between Fe^{II} and 2-MeIm of ZIF-8.

The Fe/TPTZ/ZIF-8 obtained as a powder after drying of the solution was subsequently ball milled, heated in Ar at 1050 °C for 1 h, and then heated in NH_3 at 950 °C for 15 min to yield catalyst A. Figure 3 shows the fuel-cell performance of a cathode comprising 1 $mg\,cm^{-2}$ of catalyst A. The activity at the *iR*-free cell voltage of 0.9 V (corrected for the ohmic voltage loss) was 3.5 $A\,g^{-1}$ (insert in Figure 3), and the specific current at 0.6 V (uncorrected) was 190 $A\,g^{-1}$. These values are much lower than those observed previously (12 $A\,g^{-1}$ at 0.9 V (*iR*-free) and 400–580 $A\,g^{-1}$ at 0.6 V (uncorrected)) when Fe/phen/ZIF-8 precursors with weight ratios of 1:10:90 or 1:20:80 were subjected to the same synthetic steps.[4] As a control, we also examined the fuel-cell performance of a catalyst B prepared by an identical method to that used for the synthesis of A but in the absence of TPTZ (Figure 3). Surprisingly, the curves of catalysts A and B are superimposable, as if the presence of TPTZ in the precursor of catalyst A had no effect.

These results can be understood in view of the different reactions that take place in Fe/ligand/ZIF-8 systems with TPTZ or phen ligands (Figures 1 and 2). In aqueous solution, the displacement of some Zn^{II} ions from ZIF-8 by Fe^{II} ions from $[Fe(TPTZ)_2]$ resulted in the complete insertion of Fe^{II} into ZIF-8, where it coordinates to 2-MeIm. In our catalyst precursors, ZIF-8 is in excess relative to $[Fe(TPTZ)_2]$ (the Zn/Fe molar ratio is 22:1). Such a displacement reaction between

Zn^{II} ions of ZIF-8 and di- or trivalent metal cations from an aqueous salt solution was recently reported.[11] In both catalyst precursors A and B, Fe^{II} is coordinated by 2-MeIm of ZIF-8 (see the Mössbauer spectra in Figure 2c and Figure S2), which explains the similar performance of catalysts A and B (Figure 3). The only difference in the precursor of catalyst A is the presence of either a TPTZ or $[Zn(TPTZ)_2]$ layer surrounding the ZIF-8 particles. However, during pyrolysis in Ar at 1050 °C, TPTZ and $[Zn(TPTZ)_2]$ sublime completely (see Figure S3). Not only the coordination but also the spatial positioning of Fe^{II} in the dry precursors of catalysts A and B must be similar. In the case of the precursor of catalyst B, Fe^{II} ions can readily penetrate into and react with ZIF-8 during wet impregnation. If Fe^{II} exchanged with all Zn^{II} cations situated nearest to the outer particle surface instead of diffusing into the structure, the affected ZIF-8 shell would be 3 nm thick for a 200 nm MOF particle and a Zn/Fe molar ratio of 22:1.

The theoretical minimum depth of ZIF-8 affected by Fe^{II} is thus 3 nm. However, diffusion effects are believed to establish an Fe^{II} gradient inside ZIF-8 particles. A similar mechanism leads to the dry precursor of catalyst A; this time, the Zn^{II} ions exchanged for Fe^{II} ions in ZIF-8 form a layer of $[Zn(TPTZ)_2](Ac)_2$ around Fe-doped ZIF-8 particles. The ligand TPTZ is too large to enter the ZIF-8 structure (3.4 Å aperture).

On the basis of these results, we directly ball milled the dry powders $FeAc_2$, TPTZ, and ZIF-8 (precursor of catalyst C) as a strategy to prevent the metal-ion displacement between $[Fe(TPTZ)_2]$ and ZIF-8. The absence of water should drastically reduce the rate of ion-exchange reactions, as was first verified by the long duration needed for the formation of $[Fe(TPTZ)_2]$ upon the dry ball milling of $FeAc_2$ and TPTZ (no ZIF-8). In contrast to the immediate formation of the blue complex in solution, the blue color appeared only after ball milling for 80 min. When $FeAc_2$, TPTZ, and ZIF-8 (1:10:90) were ball milled together for 3 h (precursor of catalyst C), no blue color was apparent. Nevertheless, catalyst C obtained after the heat treatment of its precursor in Ar and then NH_3 showed much improved performance (Figure 3), which was now similar to our best result obtained previously with Fe/phen/ZIF-8.[4] The apparent Tafel slopes differ slightly (68 mV dec^{-1} for catalysts A and B and 58 mV dec^{-1} for catalyst C); however, this difference is probably due to combined mass-transport and kinetic limitations in catalysts A and B even at very small currents. Micropore-hosted active sites are prone to diffusional limitations.[3a,c]

We interpret the superior performance of catalyst C relative to that of catalyst A as follows: In the former, about 1/3 of the Fe present is coordinated to TPTZ after dry ball milling (doublet d2 in Figure 2d; see also Table S1). These TPTZ-ligated ferrous ions are necessarily situated on the top surface of ZIF-8 particles, since TPTZ is too large to enter the micropores of ZIF-8. The remaining 2/3 of the Fe ions react with ZIF-8 by mechanochemistry to form the [Fe(2-MeIm)] complex (doublet d1 in Figure 2d). Doublet d1 has parameters similar to those of doublet b1 for [Fe(2-MeIm)] obtained by wet chemistry. Its appearance may be explained by localized Zn^{II}-ion displacement by Fe^{II} ions and a breakdown of the crystalline ZIF-8 structure at the outer shell into isolated [Fe(2Me-Im)] complexes. This hypothesis is supported by the much lower absorption of γ rays by the precursor of catalyst C (only 0.1 % absorption at maximum) relative to that by the precursor of catalyst A (2 % absorption; see Figure 2c,d). The probability of recoil-free γ-ray absorption by Fe^{57} nuclei is proportional to the mass of the structure that these nuclei are attached to. Hence, in the precursor of catalyst C, the iron nuclei must be bound to entities with a small mass (isolated surface complexes) rather than deeply inserted in the crystalline ZIF-8 structure. Hence, the precursor of catalyst C after dry ball milling is viewed as ZIF-8 particles surrounded by $[Fe(TPTZ)_2]$ and [Fe(2-MeIm)] complexes. The heat treatment of this precursor leads to the best-performing catalyst. The localization of Fe^{II} on the surface of ZIF-8 particles in the precursor of catalyst C is advantageous as compared to its dispersion inside ZIF-8 particles in the precursors of catalysts A and B. The pyrolysis of these different catalyst precursors leads to similar FeN_x catalytic sites, as shown by similar Mössbauer spectra (see Figure S4), but these sites are situated on average closer to the surface of the catalytic particles in catalyst C than in catalyst A and are thus more accessible to O_2 and protons, in agreement with the much improved performance of catalyst C (Figure 3).

We investigated the effect of the TPTZ/ZIF-8 ratio in the catalyst precursor and found a ratio of 10:90 to be optimal (see Figure S5). Finally, we maximized the power density in the fuel cell with catalyst C by choosing a thinner polymer membrane and setting the cathode loading to 4 mg cm^{-2} (Figure 4). With O_2, the current and power density at 0.6 V were 1.05 A cm^{-2} and 0.63 W cm^{-2}, respectively. These values are similar to those reported by us for the optimized catalyst obtained from a Fe/phen/ZIF-8 precursor: 1.25 A cm^{-2} and 0.75 W cm^{-2}, respectively. In air, the current density and power density at 0.6 V became 0.50 A cm^{-2} and 0.30 W cm^{-2}, respectively (Figure 4).

To rationalize the choice of N-containing ligands, we now demonstrate how the wet-chemistry reaction between $[Fe(TPTZ)_2]$ and ZIF-8 could have been predicted. From the definition of the formation constants, K_{f1}, K_{f2}, K_{f5}, and K_{f6}, for the complexes [Fe(2-MeIm)], [Zn(2-MeIm)], $[Fe(TPTZ)_2]$,

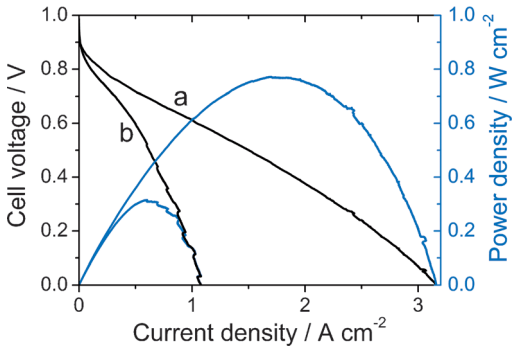

Figure 4. Polarization and power-density curves of the optimized catalyst C in a) O_2 and b) air. The cathode-catalyst loading was 4 mg cm^{-2}, and the membrane was Nafion NRE 211; otherwise, the same experimental conditions were used as described for Figure 3.

and $[Zn(TPTZ)_2]$, respectively, one can express the equilibrium constant, K_1, of the reaction:

$$[Zn(2\text{-MeIm})] + [Fe(TPTZ)_2] \Leftrightarrow [Fe(2\text{-MeIm})] + [Zn(TPTZ)_2] \quad (1)$$

as $K_1 = (K_{f1}K_{f6})/(K_{f2}K_{f5})$ (see the Supporting Information). The values for K_{f1}, K_{f2}, and K_{f5} are approximately 10^2, $10^{2.5}$, and 2×10^{10}, respectively.[12] We estimated K_{f6} by monitoring the reaction between $[Fe(TPTZ)_2]$ and Zn^{II} by UV/Vis spectroscopy (see the Supporting Information and Figure S6). The ratio K_{f6}/K_{f5} was found to be 0.3, which yields $K_{f6} = 6\times10^9$. From all these values of K_f, $K_1 = 10^{-1}$ was calculated for the equilibrium constant of Equation (1). One can then calculate that, for the catalyst precursor A, only 25% of the initial Fe^{II} ions should remain complexed with TPTZ at equilibrium; the remainder are now complexed with 2-MeIm instead. In practice, 100% of the Fe^{II} ions were complexed with 2-MeIm in the catalyst precursor A (Figure 2c). This disparity probably results from the complex solid/liquid experimental situation, which differs too strongly from the simple classical homogeneous system assumed for the calculation of the equilibrium constants. Nevertheless, the assumption of a simple classical homogeneous system enables us to explain trends and the incapacity of $[Fe(phen)_3]$ to react with ZIF-8 in our previous study with phen as a ligand. The equilibrium constant for the reaction:

$$[Zn(2\text{-MeIm})] + [Fe(phen)_3] \Leftrightarrow [Fe(2\text{-MeIm})] + [Zn(phen)_3] \quad (2)$$

is $K_2 = (K_{f1}K_{f4})/(K_{f2}K_{f3})$, in which K_{f3} and K_{f4} are the formation constants for $[Fe(phen)_3]$ and $[Zn(phen)_3]$, respectively (see the Supporting Information), and have values of 10^{21} and 10^{17}, respectively.[13] From the resulting K_2 value of $10^{-4.5}$, it may be calculated that 97% of the initial Fe ions should remain complexed with phen at equilibrium. Thus, the impregnation of ZIF-8 with $[Fe(phen)_3]$ leads to a catalyst precursor in which $[Fe(phen)_3]$ is located at the surface of ZIF-8 particles, that is, a configuration similar to that deduced for the precursor of catalyst C in this study.

In summary, the equilibrium constant K predicts whether or not the exchange of metal ions between ZIF-8 and the Fe complex will occur during the wet-impregnation step. This study reveals the detrimental effect of this cation exchange on the fuel-cell performance of Fe-based catalysts prepared from iron complexes and ZIF-8: a decrease in the power performance by a factor ≥ 2 at 0.6 V was observed when the cation-exchange reaction occurred. This aspect is important for the synthesis of non-precious-metal catalysts from iron (or cobalt) complexes and ZIF-8, and is probably transposable to other MOFs as well. Displacement between the metal–ligand complex and the MOF is of the greatest importance in the generic synthetic approach with MOFs: an approach that has been successful for the generation of nanostructured oxide, nitride, and carbide materials.[6]

Received: April 11, 2013
Published online: May 29, 2013

Keywords: chelates · fuel cells · iron · UV/Vis spectroscopy · zeolites

[1] a) L. Schlapbach, *Nature* **2009**, *460*, 809; b) J. Tollefson, *Nature* **2010**, *464*, 1262.
[2] B. D. James, J. A. Kalinoski, K. N. Baum, **2008**, in *U.S. Department of Energy—Hydrogen Program, 2008 Annual Progress Report*, http://www.hydrogen.energy.gov/pdfs/progress08/v_a_2_james.pdf.
[3] a) M. Lefèvre, E. Proietti, F. Jaouen, J. P. Dodelet, *Science* **2009**, *324*, 71; b) G. Wu, K. L. More, C. M. Johnston, P. Zelenay, *Science* **2011**, *332*, 443; c) F. Jaouen, E. Proietti, M. Lefèvre, R. Chenitz, J. P. Dodelet, G. Wu, H. T. Chung, C. M. Johnston, P. Zelenay, *Energy Environ. Sci.* **2011**, *4*, 114; d) G. Wu, K. Artyushkova, M. Ferrandon, A. J. Kropf, D. Myers, P. Zelenay, *ECS Trans.* **2009**, *25*, 1299; e) S.-T. Chang, C.-H. Wang, H.-Y. Du, H.-C. Hsu, C.-M. Kang, C.-C. Chen, C.-S. Wu, S.-C. Yen, W.-F. Huang, L.-C. Chen, M.-C. Lin, K.-H. Chen, *Energy Environ. Sci.* **2012**, *5*, 5305.
[4] E. Proietti, F. Jaouen, M. Lefèvre, N. Larouche, J. Tian, J. Herranz, J. P. Dodelet, *Nat. Commun.* **2011**, *2*, 416.
[5] a) G. Goenaga, S. Ma, S. Yuan, D. J. Liu, *ECS Trans.* **2010**, *33*, 579; b) S. Ma, G. A. Goenaga, A. V. Call, D. J. Liu, *Chem. Eur. J.* **2011**, *17*, 2063; c) D. Zhao, J. L. Shui, C. Chen, X. Chen, B. N. Reprogle, D. Wang, D. J. Liu, *Chem. Sci.* **2012**, *3*, 3200.
[6] a) A. Morozan, F. Jaouen, *Energy Environ. Sci.* **2012**, *5*, 9269; b) S. L. Li, Q. Xu, *Energy Environ. Sci.* **2013**, *6*, 1656.
[7] a) C. Bezerra, L. Zhang, K. Lee, H. Liu, J. Zhang, Z. Shi, A. Marques, E. Marques, S. Wu, *Electrochim. Acta* **2008**, *53*, 7703; b) L. Zhang, K. Lee, C. W. B. Bezerra, J. Zhang, J. Zhang, *Electrochim. Acta* **2009**, *54*, 6631; c) A. Velázquez-Palenzuela, L. Zhang, L. Wang, P. L. Cabot, E. Brillas, K. Tsay, J. Zhang, *Electrochim. Acta* **2011**, *56*, 4744.
[8] L. Kukoc-Modun, N. Radić, *Croat. Chem. Acta* **2010**, *83*, 189.
[9] N. Mudasir, N. Yoshioka, H. Inoue, *Transition Met. Chem.* **1999**, *24*, 210.
[10] a) D. Sedney, M. Kahjehnassiri, W. M. Reiff, *Inorg. Chem.* **1981**, *20*, 3476; b) C. R. Johnson, R. E. Shepherd, *Inorg. Chem.* **1983**, *22*, 3506.
[11] L. Zhang, Y. H. Hu, *J. Phys. Chem. C* **2011**, *115*, 7967.
[12] a) L. E. Kapinos, B. Song, H. Sigel, *Inorg. Chim. Acta* **1998**, *280*, 50; b) E. B. Buchanan, Jr., D. Crichton, J. R. Bacon, *Talanta* **1966**, *13*, 903.
[13] a) C. V. Banks, R. I. Bystroff, *J. Am. Chem. Soc.* **1959**, *81*, 6153; b) J. M. Dale, C. V. Banks, *Inorg. Chem.* **1963**, *2*, 591.

